J. Fluid Mech. (2002), *vol.* 471, *pp.* 203–217. © 2002 Cambridge University Press
DOI: 10.1017/S0022112002002069 Printed in the United Kingdom

Slow mixed convection in rectangular containers

By P. N. SHANKAR[1], V. V. MELESHKO[2] AND E. I. NIKIFOROVICH[2]

[1]Computational and Theoretical Fluid Dynamics Division, National Aerospace Laboratories, Bangalore 560017, India

[2]Institute of Hydromechanics, National Academy of Sciences, 252057 Kiev, Ukraine

(Received 11 March 2002 and in revised form 26 June 2002)

We consider the slow motion of viscous fluid completely filling a rectangular container. The motion is generated by the combined action of differential wall temperatures and the linear motion of the lid. If the relevant Reynolds and Péclet numbers and the lid speed are all small enough, the velocity field will be governed by an inhomogeneous biharmonic equation. In this approximation the temperature field, unaffected by the fluid motion, drives, at least in part, the fluid velocity field. Of interest here are the relative effects of buoyancy and lid motion. It is shown that the field, suitably scaled, depends on the dimensionless depth and lid speed alone. The mixed convection problem is solved for two pairs of wall heating protocols by sequentially solving, by an eigenfunction expansion method, up to four biharmonic problems. We present streamline patterns and quantitative data on the relative effects of lid motion on the buoyancy-driven fields in these containers.

1. Introduction

We are concerned in this paper with fluid motions in rectangular containers which are induced, possibly simultaneously, by both buoyancy and the motion of the lid of the container. The motivation, although this aspect will not be pursued very far here, is that the fluid motion caused by one of the agents may possibly be controlled by the effective use of the other. There are a number of materials processing systems in which buoyancy-driven fluid motions play a critical role (Jaluria 2001). For example, the flows that arise in molten crystals strongly affect the quality of the crystals that are obtained and hence of the semiconductors fabricated from them. In casting processes, buoyancy-driven flows in the liquid melt can seriously influence the microstructure of the casting. The present investigation yields qualitative and quantitative data on flows which model these processes well and suggests a method for their control.

We will assume in this investigation that the temperature differences are small enough and the fluid thermal conductivity high enough that to a first approximation the temperature field is unaffected by the fluid motion; the latter will be assumed slow enough that inertial effects can be consistently ignored in this approximation.

Viscous liquid completely fills a rectangular container of lateral width $\tilde{A}$ and depth $\tilde{D}$. The container walls are maintained at constant but not necessarily uniform temperatures $\tilde{T}_T$, $\tilde{T}_R$, $\tilde{T}_B$ and $\tilde{T}_L$ respectively while the lid moves at constant speed $\tilde{V}_0(y)$ in the y-direction; gravity acts downwards in the positive x-direction. If the four wall temperatures are not uniform and equal, density variations in the liquid caused by gradients in the temperature will induce slow fluid motion even if the lid

https://doi.org/10.1017/S0022112002002069 Published online by Cambridge University Press

is stationary. In this framework the questions we wish to address are: (i) how does the primary eddy system depend on the type of wall heating that is applied, (ii) are there corner eddies and if so at which corners and how are they affected by the wall heating and (iii) how do changing the cavity depth $\tilde{D}$ and the lid velocity $\tilde{V}_0$ modify the eddy structure in the cavity?

A few papers have appeared in the literature which consider buoyancy-driven Stokes flows in frameworks similar to the one we consider here. In a 1975 paper Joseph & Sturges calculate, using domain perturbation theory, the shape of the free surface of a liquid in a trench subjected to sidewall heating. The free-surface problem is particularly suited to the application of biorthogonality relations to the relevant biharmonic eigenfunctions and Joseph & Sturges exploit this. For an infinitely deep trench with one of the sidewalls heated and the top insulated, the coefficients in the expansion for the stream function can be found explicitly; they find a single primary eddy in the trench. The same result is found for trenches of finite depth with the bottom also insulated; in this case however the biorthogonality relations lead to an infinite system of equations for the coefficients which need to be solved by truncation. For trenches of finite depth Joseph & Sturges are silent on the issue of the existence of corner eddies at the bottom corners. Liu & Joseph (1977) extended this analysis, using the same techniques, to similar motions in wedge-shaped trenches. Here, however, they explicity point out the absence of corner eddies at the apex of the wedge, correcting a commonly held but incorrect view that such eddy systems must always exist at all sharp corners. In the thermally driven flow considered by Liu & Joseph the outer flow generated by the particular solution dominates the corner or edge eddies generated by the complex eigenfunctions of the homogeneous solution, leading to a suppression of the corner eddy system. Yu & Nansteel (1990), however, show that if the wedge angle is between approximately 126° and 146° corner eddies may be present near the apex if the top boundary is of the no-slip rather than the free-shear type.

While the present work also considers buoyancy-driven creeping motions, it is quite different from the above studies both in motivation and the type of results obtained. Our motivation is in estimating to what extent the lid motion can modify the flow structure set up by thermal convection. This aspect was not considered in the earlier investigations. Moreover, we will show that even the primary eddy structure can be very different from the very simple unicellular structures seen earlier. This is because temperature boundary conditions on all four walls, rather than adiabatic conditions on one or a pair of walls as in the earlier studies, can lead to far more complex temperature fields and consequently to more complex convection fields. It will also be shown that corner eddies may, indeed, be present in these buoyancy-driven motions.

2. Formulation and analysis

We assume the rectangular container to be completely filled with a Newtonian fluid whose coefficient of thermal expansion β is small. We also assume that all fluid properties are constant. Let $\tilde{T}_0$ be a constant reference temperature and let β be the coefficient of thermal expansion about this temperature. In the problems that we will be considering there is a wall temperature scale $\tilde{T}_1$ ($> \tilde{T}_0$) and consequently a temperature difference $\Delta\tilde{T}_0 = \tilde{T}_1 - \tilde{T}_0$. It will prove convenient to work with the dimensionless temperature θ defined by $\theta = (\tilde{T} - \tilde{T}_0)/(\tilde{T}_1 - \tilde{T}_0)$. Let us now choose the container width $\tilde{A}$ and the reference density $\tilde{\rho}_0$ as the scales for length and density

https://doi.org/10.1017/S0022112002002069 Published online by Cambridge University Press

respectively and define

$$\tilde{q}_0 = g\tilde{\rho}_0\tilde{A}^2\beta\Delta\tilde{T}_0/\mu \tag{1}$$

as the velocity scale. Having chosen these, the scales for the time and pressure are $\tilde{t}_0 = \tilde{A}/\tilde{q}_0$ and $\tilde{p}_0 = \mu\tilde{q}_0/\tilde{A}$.

If the differential heating on the walls is not too large, we can treat the fluid as incompressible with the density changes affecting the buoyancy alone. In the Boussinesq approximation (Chandrasekhar 1961), the two-dimensional equations of continuity, momentum, energy and state take the form

$$\nabla\cdot\boldsymbol{v} = 0, \tag{2a}$$

$$(1-\beta\Delta\tilde{T}_0\theta)\,Re\,\frac{\mathrm{D}\boldsymbol{v}}{\mathrm{D}t} = -\nabla p - \theta\hat{\boldsymbol{e}}_x + \nabla^2\boldsymbol{v}, \tag{2b}$$

$$(1-\beta\Delta\tilde{T}_0\theta)\,Pe\,\frac{\mathrm{D}\theta}{\mathrm{D}\tilde{t}} = -\tilde{\nabla}^2\theta, \tag{2c}$$

$$\rho = 1-\beta\Delta\tilde{T}_0\theta, \tag{2d}$$

where the tilde-less quantities are the dimensionless field variables. In the above, p is the pressure over and above the hydrostatic pressure, $Re = \tilde{\rho}_0\tilde{q}_0\tilde{A}/\mu$ is the Reynolds number and $Pe = \tilde{\rho}_0 c_p\tilde{q}_0\tilde{A}/k$ is the Péclet number relevant to this buoyancy-driven field. In this paper we are primarily interested in the situation where the steady fluid motion is slow enough and the fluid thermal conductivity high enough that the inertial terms in both the momentum and energy equations can be neglected. More precisely we allow $Re\to 0$ and $Pe\to 0$ in equations (2); moreover, in the mixed convection case we will assume $V_0 < q_0$ so that these dimensionless quantities when based on the lid velocity will also be vanishingly small. Under these circumstances the governing field equations reduce to the linear system

$$\nabla\cdot\boldsymbol{v} = 0, \tag{3a}$$

$$\nabla^2\boldsymbol{v} = \nabla p + \theta\hat{\boldsymbol{e}}_x, \tag{3b}$$

$$\nabla^2\theta = 0. \tag{3c}$$

Eliminating the continuity equation through the use of a stream function $\psi(x,y)$, $u = \psi_y$, $v = -\psi_x$, we obtain a single equation for the stream function

$$\nabla^4\psi = \theta_y. \tag{4}$$

Thus the velocity field is governed by an inhomogeneous biharmonic equation which shows that, boundary forcing apart, the field is driven by the known temperature field.

Before considering the boundary conditions that will come into play let us define a symmetric function $f(x;D,\delta)$ on $[-D/2, D/2]$ by

$$f(x;D,\delta) = \begin{cases} 1 & 0 \leqslant |\,x\,| \leqslant (D/2-\delta D) \\ 0.5\{1+\cos[\pi(x-(D/2-\delta D))/\delta D]\} & (D/2-\delta D) < |\,x\,| \leqslant D/2. \end{cases} \tag{5}$$

If δ is small the function is equal to 1 over most of the interval and then falls smoothly to 0 near the end points. We shall in this paper be considering four types of wall temperature protocols:

Case A: left-hand wall heated and the other walls at ambient, i.e. $\theta_L = f(D/2-x; D,\delta)$, $\theta_R = \theta_T = \theta_B = 0$;

https://doi.org/10.1017/S0022112002002069 Published online by Cambridge University Press

Case B: left-hand wall heated, right-hand wall cooled and the other walls at ambient, i.e. $\theta_L = -\theta_R = f(D/2 - x; D, \delta)/2$, $\theta_T = \theta_B = 0$;

Case C: top wall heated and the other walls at ambient, i.e. $\theta_T = f(y; 1, \delta), \theta_R = \theta_L = \theta_B = 0$;

Case D: top wall heated, bottom wall cooled and the other walls at ambient, i.e. $\theta_T = -\theta_B = f(y; 1, \delta)/2$, $\theta_R = \theta_L = 0$.

We shall always take the velocity of the lid to be given by $v(0, y) = V_0(0, y) = v_0 f(y; 1, \delta)$ where v_0 is a constant. It should be noted that we have chosen all boundary data to be continuous and smooth. This is not essential as is known from Srinivasan (1995), Meleshko (1996) and the discussion in Shankar & Deshpande (2000). Our choice here has been made so that convergence of all relevant series will be more rapid than if the boundary data were non-smooth or discontinuous.

Each in the pairs (A,B) and (C,D) seem so similar that it may seem sufficient to consider one in each pair alone. But we shall show in what follows that there are surprising differences in the flow fields. In order to keep the number of parameters at a minimum all the results here have been obtained with $\delta = 0.1$.

We shall now outline the procedure used to solve the mixed-convection problems formulated above. Specifically this will be done for Case C with the understanding that the same procedure applies to the other cases with only minor differences in the details. If the top wall alone is heated, it is easy to show that the temperature field has the Fourier series representation

$$\theta(x, y) = \sum_{n=1}^{\infty} \gamma_n \frac{\sinh \sigma_n (D - x)}{\sinh \sigma_n D} \cos \sigma_n y, \tag{6}$$

where $\sigma_n = (2n - 1)\pi$, $\gamma_n = \hat{\gamma}(n, \delta)$ and $\hat{\gamma}(n, \delta)$ are the Fourier coefficients of $f(x; D, \delta)$. From (4) the stream function $\psi(x, y)$ now has to satisfy the inhomogeneous biharmonic equation

$$\nabla^4 \psi = -\sum_{n=1}^{\infty} \gamma_n' \sinh \sigma_n (D - x) \sin \sigma_n y, \tag{7}$$

where $\gamma_n' = \gamma_n \sigma_n / \sinh \sigma_n D, n = 1, 2, 3, \ldots$.

We will require the stream function $\psi(x, y)$ to vanish on all four walls of the container and the tangential velocity to vanish on the sidewalls and the bottom wall; on the top wall we require the v-component of the fluid velocity to equal the lid speed.

First we write down a solution $\psi^i(x, y)$ of the inhomogenous equation (7):

$$\psi^i(x, y) = -\sum_{n=1}^{\infty} \frac{\gamma_n'}{8\sigma_n^2} x^2 \sinh \sigma_n (D - x) \sin \sigma_n y. \tag{8}$$

If we now write $\psi = \psi^i + \psi^h$, ψ^h has now to be biharmonic and the problem has been reduced to one of finding a biharmonic function in the rectangle satisfying given boundary data. Among the methods suggested in the literature for solving the biharmonic problem in the rectangle we mention the use of biorthogonal series (Joseph & Sturges 1975), the use of boundary integrals (Pozrikidis 1994), the superposition method (Meleshko 1996) and direct numerical computation (Pan & Acrivos 1967; Tuann & Olson 1978). However, since the geometry here is a simple one and we wish to keep the numerical work to a minimum the direct eigenfunction expansion method

https://doi.org/10.1017/S0022112002002069 Published online by Cambridge University Press

seems to be particulary suitable. The procedure followed in Shankar (1993) is utilized here and the reader is referred to that paper for details.

We write ψ as the sum of the above inhomogeneous solution and a pair of biharmonic functions, $\psi = \psi^i + \psi^1 + \psi^2$, i.e. $\nabla^4\psi^1 = \nabla^4\psi^2 = 0$. Moreover, ψ^1 and ψ^2 each satisfy homogeneous boundary conditions on pairs of walls, $\psi^1 = \psi^1_y = 0$ on $y = \pm\frac{1}{2}$ and $\psi^2 = \psi^2_x = 0$ on $x = 0$ and $x = D$.

Recall the biharmonic eigenfunctions related to symmetric and skew-symmetric velocity fields respectively (Moffatt 1964): $\phi^{\pm}_s(x, y) = \{y \cos \lambda_s y - \frac{1}{2}\cot(\lambda_s/2)\sin\lambda_s y\}\exp \pm \lambda_s x$ and $\phi^{\pm}_a(x, y) = \{y \sin \lambda_a y - \frac{1}{2}\tan(\lambda_a/2)\cos\lambda_a y\}\exp \pm\lambda_a x$ where where the eigenvalues λ_s and λ_a satisfy $\sin\lambda_s = \lambda_s, \sin\lambda_a = -\lambda_a$ respectively.

The idea now is to write ψ^1 as the sum of parts symmetric and skew-symmetric in y respectively and ψ^2 as the sum of parts symmetric and skew-symmetric in $D/2 - x$ respectively, i.e. $\psi = \psi^1_s + \psi^1_a + \psi^2_s + \psi^2_a$. We can now formally expand ψ^1_s and ψ^1_a as follows:

$$\psi^1_s(x, y) = \mathrm{Re}\sum_n \{a_n\phi^+_s(x, y) + b_n\phi^-_s(x, y)\}, \tag{9a}$$

$$\psi^1_a(x, y) = \mathrm{Re}\sum_n \{c_n\phi^+_a(x, y) + d_n\phi^-_a(x, y)\}, \tag{9b}$$

in terms of the symmetric and skew-symmetric eigenfunctions respectively. If the boundary conditions on ψ^1 are now decomposed into parts symmetric and skew-symmetric in y the boundary conditions required on ψ^1_s and ψ^1_a will be obtained. The unknown complex coefficients a_n, b_n, c_n and d_n can then be obtained by the least-squares procedure suggested in Shankar (1993). The method has been shown to work accurately and efficiently on a number of different Stokes flow problems (Shankar & Deshpande 2000). The same procedure can be applied to ψ^2_s and ψ^2_a.

It should be noted that, as formulated here, there are only two physical parameters that affect the field, the depth D and the lid speed v_0.

3. Discussion of the results

First, we applied the present method to the problem considered by Joseph & Sturges (1975). Here the right-hand wall is hotter than the left-hand wall while the top and bottom walls are insulated. In this case $\theta(x, y) = 0.5 + y$ and so we can take $\psi^i(x, y) = x^4/24$ and go through the suggested procedure with $v_0 = 0$, since here we are only considering natural convection. As found earlier by Joseph & Sturges, we find for all depths that there is a single primary eddy with no apparent fine structure in it. However, we do find corner eddies at all four corners of the container because of the much larger number eigenfunctions that we have used (200 as against 9); the primary interest in Joseph & Sturges (1975) was in computing the free surface of the liquid not in the corner eddies. In what follows we will concentrate on the four cases enumerated in § 2. We dispose of the less interesting Cases A and B first before dealing with the more interesting Cases C and D.

3.1. *Sidewall heating, Cases A and B*

If the left-hand wall alone is heated, the temperature field has the Fourier series representation

$$\theta(x, y) = \sum_{n=1}^{\infty} \gamma_n \sinh\sigma_n(0.5 - y)\cos\sigma_n(x - D/2)/\sinh\sigma_n,$$

https://doi.org/10.1017/S0022112002002069 Published online by Cambridge University Press

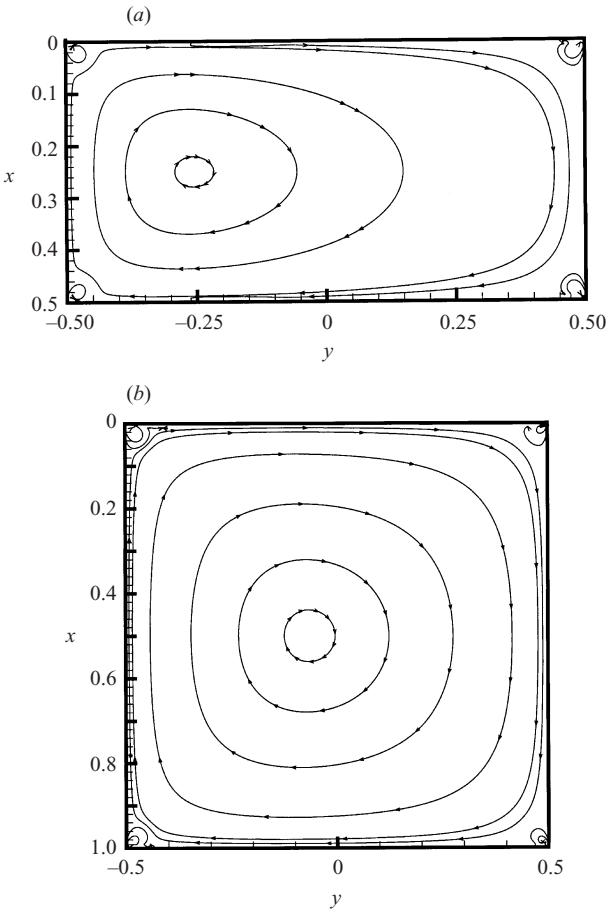


FIGURE 1. Buoyancy-induced convection when the left-hand wall alone is heated and the other three walls are at ambient temperature (Case A). (*a*) $D = 0.5$ and (*b*) $D = 1$.

where $\sigma_n = (2n-1)\pi/D$, $\gamma_n = \hat{\gamma}(n, \delta)$ while the inhomogeneous solution is given by

$$\psi^i(x, y) = -\sum_{n=1}^{\infty} \gamma_n y^2 \cosh \sigma_n(0.5 - y) \cos \sigma_n(x - D/2)/8\sigma_n \sinh \sigma_n.$$

A check on the boundary conditions reveals that ψ^2 is symmetric about $x = D/2$ and hence ψ_a^2 is superfluous in this case – we need only carry out three biharmonic calculations. Figure 1 shows the streamline patterns of natural convection ($v_0 = 0$) for containers of depth 0.5 and 1; calculations for deeper and shallower containers show the same pattern. In all cases there is a single primary eddy with the fluid moving upwards near the hot wall and returning, as might be expected, downwards near the cold right-hand wall. For small depths the centre of the primary eddy is always closer to the hot wall but, again as might be expected, it moves closer and closer to the centreline as the depth increases; note that there is no symmetry about the mid-plane $y = 0$. Now one would also expect the effect of the hot left-hand wall in driving the circulation to increase as the depth increases. This is seen quantitatively in table 1 which shows that the magnitude of the stream function near the eddy centre does indeed increase with depth.

https://doi.org/10.1017/S0022112002002069 Published online by Cambridge University Press

Depth D	Case A	Case B	Case C	Case D
0.25			1.129×10^{-5}	3.848×10^{-4}
0.5	1.533×10^{-4}	8.497×10^{-5}	7.345×10^{-5}	7.199×10^{-4}
1	1.085×10^{-3}	1.052×10^{-3}	1.666×10^{-4}	1.199×10^{-3}
2	2.466×10^{-3}	2.465×10^{-3}	1.718×10^{-4}	1.477×10^{-3}
4	2.607×10^{-3}	2.607×10^{-3}	1.718×10^{-4}	1.492×10^{-3}

TABLE 1. Stream function magnitudes $|\psi|$ at the centres of the primary eddies in buoyancy-driven convection.

Of interest is the fact that corner eddies are visible at all the corners and for all depths. It should be noted that the velocity field can be conveniently thought of as being a superposition of a flow induced by the buoyancy and a field generated by the complex eigenfunctions needed to eliminate the induced field on the boundaries. Now the latter have the potential to both generate primary eddies in deep cavities (Shankar 1993) and generate corner eddies. In this case, new primary eddies are not generated because the non-decaying real inhomogeneous field always dominates, in the core of the flow, the decaying field generated by the complex eigenfunctions. However, near all the corners, in this case, the roles are reversed and the corner eddies appear.

The possibility of controlling these flows is illustrated in figure 2 for the case of a cavity of depth 0.5. The circulation set up by natural convection is clockwise and we might ask how fast must the lid move to the left in order to significantly reduce the natural circulation. It can be seen from the figure that the moving lid generates an eddy, initially centred near the right-hand wall, which gradually penetrates the cavity as the lid speed increases. Whereas the corner eddy at the top right disappears immediately, the one at the top left appears to become a free eddy while gradually losing its strength. We observe that whereas most of the field is similar to one associated with a flow driven by the lid alone when $v_0 = -0.01$, the thermal primary eddy is still there near the left-hand corner. The maximum fluid speed in thermal convection alone is of the order of 0.001; note that even when there is a significant counter-circulation driven by the lid ($v_0 = -0.001$) the thermally driven convection near the eddy centre is hardly affected.

In Case B, the left-hand wall is heated and the right-hand wall cooled while the net temperature difference between the left-hand wall and the right-hand wall is the same as in Case A; but now the temperatures of the top and bottom walls are a mean of those of the sidewalls. The temperature field is now given by

$$\theta(x, y) = \sum_{n=1}^{\infty} \gamma_n \sinh \sigma_n y \cos \sigma_n (x - D/2)/\sinh \sigma_n/2,$$

where $\sigma_n = (2n-1)\pi/D$, $\gamma_n = -\hat{\gamma}(n, \delta)/2$; the inhomogeneous solution in this case is given by

$$\psi^i(x, y) = \sum_{n=1}^{\infty} \gamma_n y^2 \cosh \sigma_n y \cos \sigma_n (x - D/2)/8\sigma_n \sinh (\sigma_n/2).$$

Examination of the boundary conditions reveals that there is even greater symmetry in this case than obtained in A. In fact we only need the symmetric parts of ψ^1 and ψ^2 and consequently one needs to only solve two, rather than four, biharmonic problems to resolve the mixed convection problem. The streamline patterns in natural

https://doi.org/10.1017/S0022112002002069 Published online by Cambridge University Press

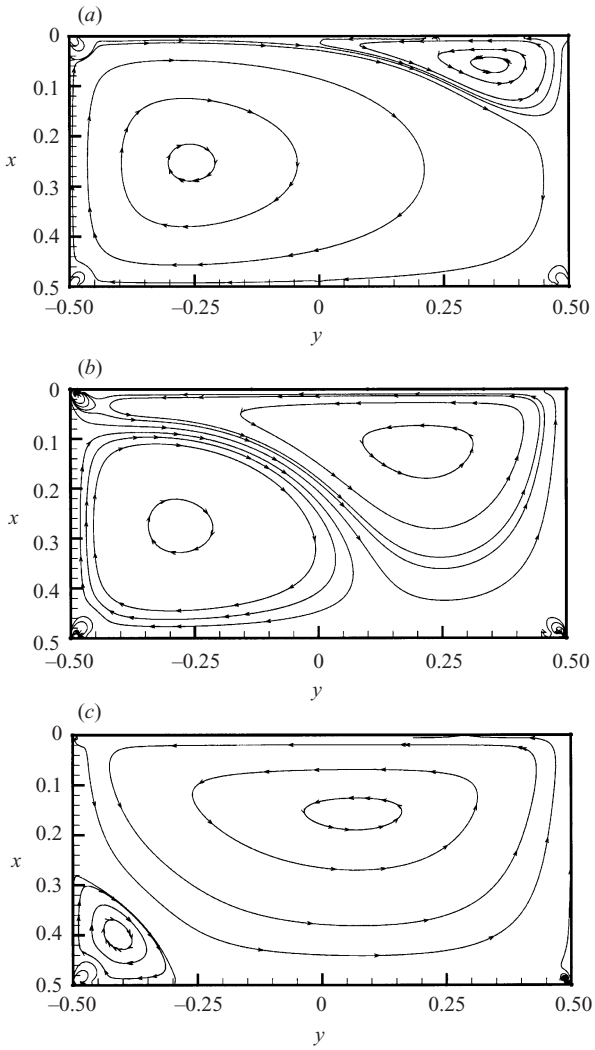


FIGURE 2. Mixed convection in a cavity of depth $D = 0.5$ when the left-hand wall alone is heated. (*a*) $v_0 = -0.0001$, (*b*) $v_0 = -0.001$ and (*c*) $v_0 = -0.01$.

convection, i.e. with $v_0 = 0$, are shown in figure 3 for $D = 0.5$ and $D = 1$; for greater depths the structure is as in the square case. In the latter cases, as expected there is a single primary eddy in each case with the eddy centre at the geometric centre of the container. However, there is a surprise: in the case of a shallow container of depth 0.5 the primary eddy, rather than being a simple centre, has additional structure. The primary eddy contains two sub-eddies whose centres are connected by a saddle. Also, as in A there are corner eddies at all four corners.

The case of mixed convection in the shallower cavity is illustrated in figure 4. The extra symmetry in this case seems to lead to some differences from what was seen in figure 2. At the lowest speed considered the lid-driven circulation displays two centres connected by a saddle as opposed to a single unsymmetrically placed centre seen in figure 2. Although these are not resolved fully here, there are symmetrically placed free eddies at the upper corners, and corner eddies at the lower corners. When the lid

https://doi.org/10.1017/S0022112002002069 Published online by Cambridge University Press

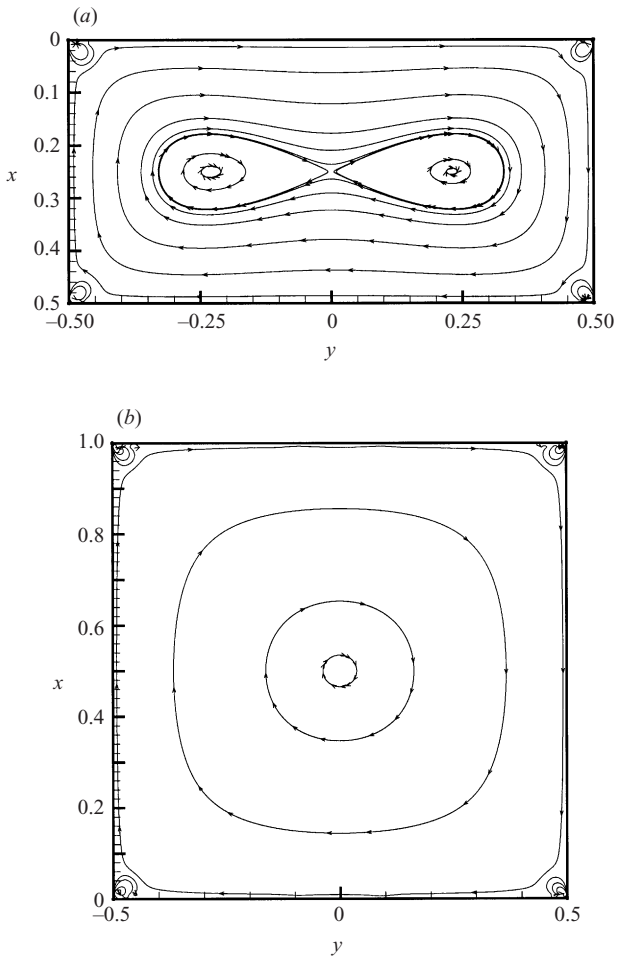


FIGURE 3. Streamline patterns in buoyancy-induced convection when the left-hand wall is heated and the right-hand wall cooled with respect to the top and bottom walls (Case B). (*a*) $D = 0.5$ and (*b*) $D = 1$.

speed is increased, we see in frame (*b*) that the circulatory region near the lid contains a single centre but the free eddies near the upper corners remain. The latter appear to have finally disappeared in frame (*c*), but even here, where the flow resembles that due to the lid motion alone over most of the field, the thermal eddies remain near the lower corners.

3.2. *Top and bottom wall heating, Cases C and D*

The details of Case C were discussed in § 2, where the temperature field was given by (6) while an inhomogeneous solution was displayed in (8). Unlike the previous cases, the solution of the mixed-convection problem requires the solution of all four biharmonic problems.

We begin by looking at the streamline patterns in buoyancy-induced convection alone, figure 5. For all depths we have two counter-rotating primary eddies. This is to be expected since the boundary conditions are symmetric about $y = 0$. As in the previously considered cases the real inhomogeneous field does not decay exponentially

https://doi.org/10.1017/S0022112002002069 Published online by Cambridge University Press

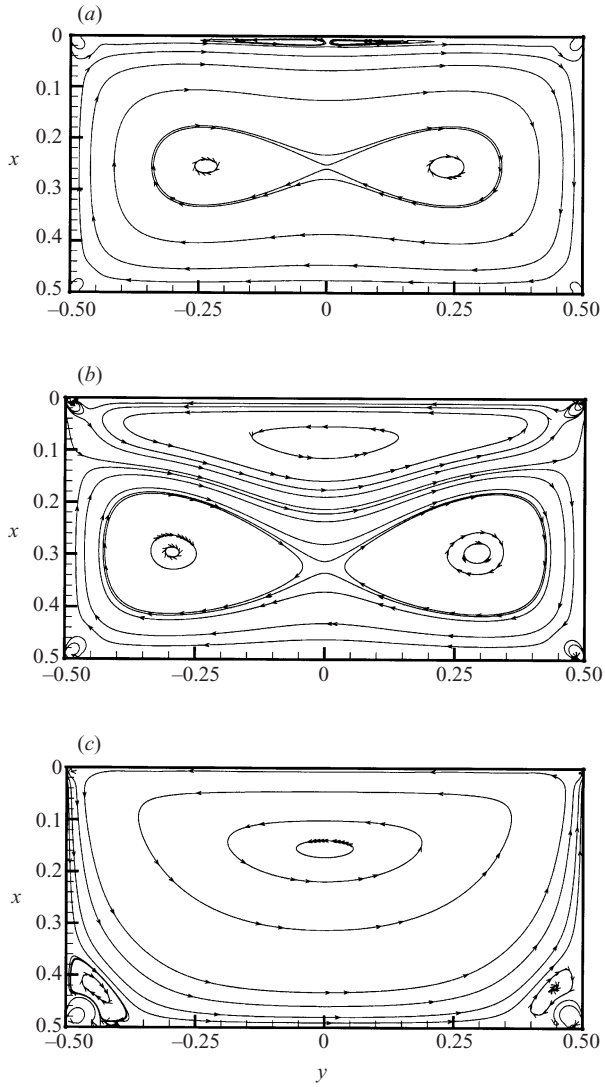


FIGURE 4. Mixed convection in a cavity of depth $D = 0.5$ when the left-hand wall is heated and the right cooled with respect to the top and bottom walls. (*a*) $v_0 = -0.0001$, (*b*) $v_0 = -0.001$ and (*c*) $v_0 = -0.01$.

with depth and so it dominates the contribution from the complex eigenfunctions; as a result we do not find more primary eddies with increasing depth. A new feature here is that we find corner eddies only at the bottom corners; either they do not exist at the top corners or they are too small there to be resolved with this level of effort.

How does the strength of the circulation depend on the depth? If we go back to table 1. we observe that the magnitude of ψ at the eddy centre is generally an increasing function of depth. This can be understood if we recall that if the sidewalls were infinitely far away the initial stratification would be stable and there would be no flow whatsoever. The flow takes place only because there are cooler sidewalls and the closer they are the greater would be the circulation.

Mixed convection in a cubical cavity with a hot top lid is considered in figure 6.

https://doi.org/10.1017/S0022112002002069 Published online by Cambridge University Press

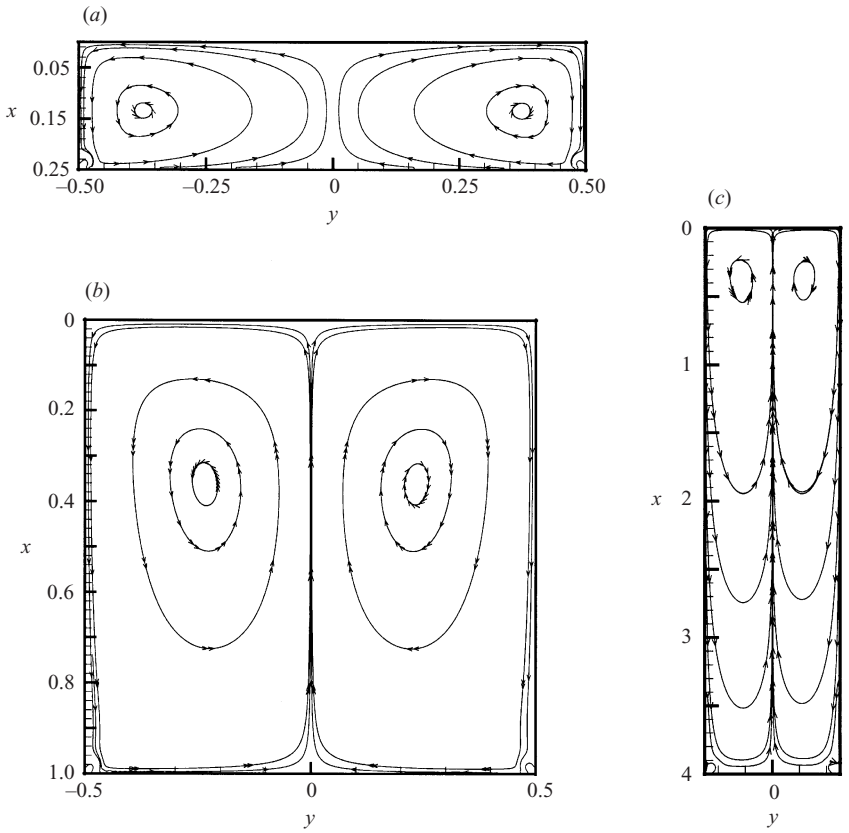


FIGURE 5. Streamline patterns in buoyancy-induced convection when the top wall alone is heated and the others are at ambient temperature (Case C). (*a*) $D = 0.25$, (*b*) $D = 1$ and (*c*) $D = 4$.

There are no surprises here: the lid-driven circulation simply enhances one of the counter-rotating thermal eddies while diminishing the other. With increasing lid speed the enhanced eddy moves to the centreline while the other is compressed into one corner.

In Case D the top wall is heated and the bottom wall cooled with respect to the sidewalls. As a consequence, unlike in Case C, the stream function in natural convection has to be antisymmetric about $x = D/2$ also. This can also be inferred from equation (4). The temperature field is now given by

$$\theta(x, y) = \sum_{n=1}^{\infty} \gamma_n \sinh \sigma_n(D/2 - x) \cos \sigma_n y / \sinh \sigma_n D/2,$$

where $\sigma_n = (2n - 1)\pi$, $\gamma_n = \hat{\gamma}(n, \delta)/2$. A suitable inhomogeneous solution, with the right symmetry, for this case is

$$\psi^i(x, y) = \sum_{n=1}^{\infty} \gamma'_n y^2 \sin \sigma_n y \sinh \sigma_n(D/2 - x)/8\sigma_n^2,$$

where the γ'_n are scalars.

The streamline patterns in buoyancy-induced convection are shown in figure 7. We now have symmetry about both vertical and horizontal mid-planes and so generally

https://doi.org/10.1017/S0022112002002069 Published online by Cambridge University Press

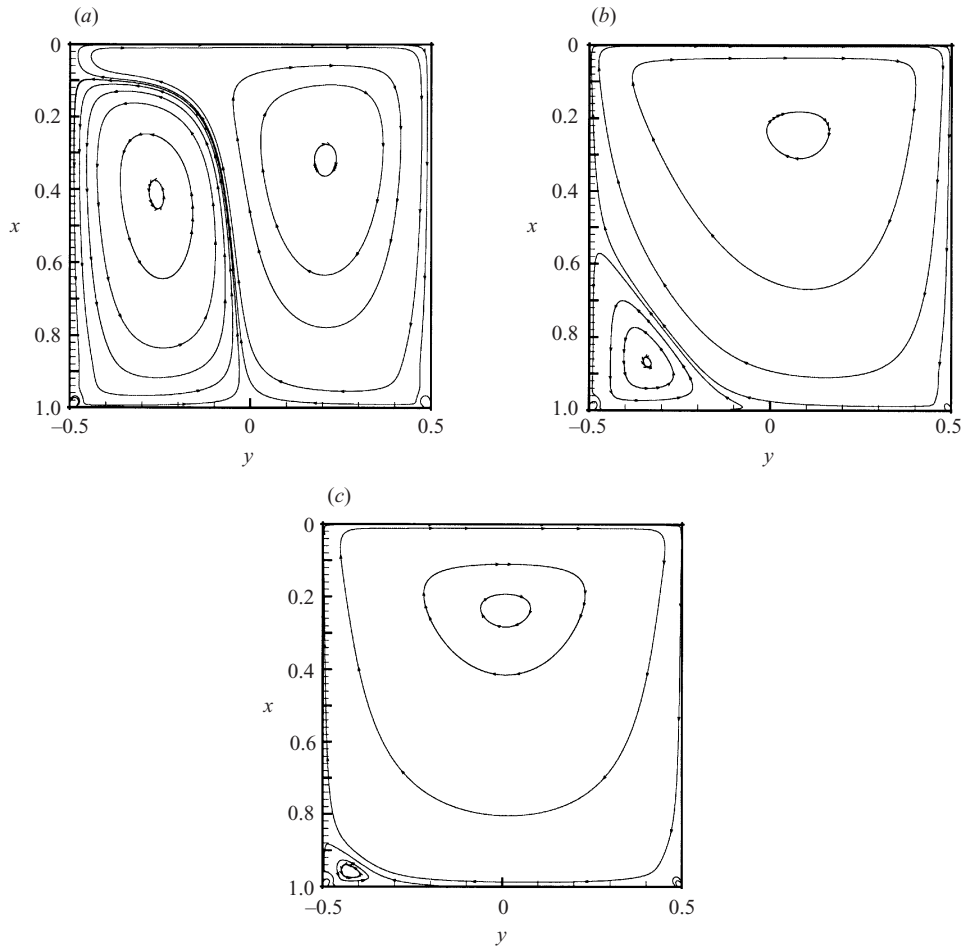


FIGURE 6. Mixed convection in a cavity of unit depth when the top wall alone is heated. (*a*) $v_0 = 0.001$, (*b*) $v_0 = 0.01$ and (*c*) $v_0 = 0.1$.

there are four counter-rotating eddies. How the eddy strengths vary with depth can be inferred from the values of $|\psi|$ at the eddy centres given in table 1: as in Case C these values increase with depth though the levelling off is slower. Note also that the magnitudes are generally about an order of magnitude larger. Another difference is the absence of corner eddies; they are either very weak or absent in this case. The shallow container of depth 0.25 displays a feature not seen in the other cases: the appearance of two more pairs of counter-rotating eddies near the centre of the container. These are much weaker than the ones near the sidewall, the maximum $|\psi|$ values being about 6.5×10^{-8} as opposed to about 3.5×10^{-4} near the sidewalls. As the container depth becomes smaller and smaller we would expect the field near the vertical centreplane to approximate that of the quiescent field in a stably stratified liquid. Figure 7(*a*) shows that this will be achieved by having a series of very weak eddies away from the sidewalls together with the relatively stronger sidewall eddies confined to the neighbourhood of the sidewalls.

Mixed convection in a shallow container of depth 0.25 is displayed in figure 8. Even at very low lid speeds the four-celled topology seen in the previous figure is

https://doi.org/10.1017/S0022112002002069 Published online by Cambridge University Press

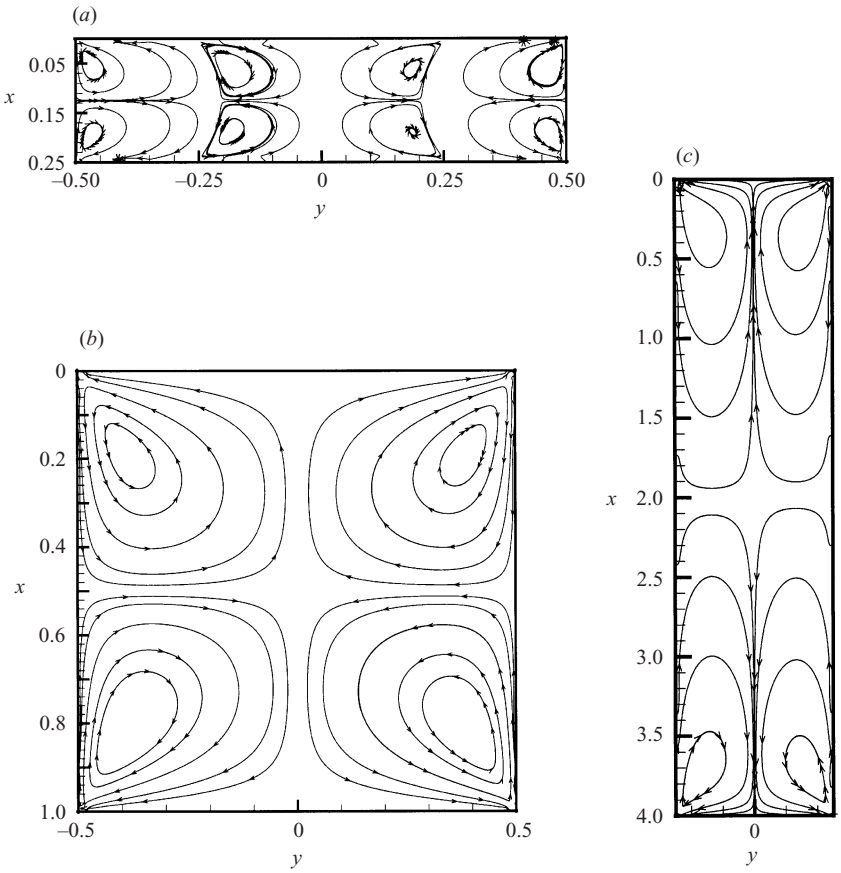


FIGURE 7. Streamline patterns in buoyancy-induced convection when the top wall is heated and the bottom wall cooled with respect to the sidewalls at ambient temperature (Case D). (*a*) $D = 0.25$, (*b*) $D = 1$ and (*c*) $D = 4$.

changed considerably. As seen in panel (*a*), in order to accommodate the lid-driven circulation the cells on the upper right and the lower left combine to form a single eddy containing both centres but now connected by a saddle. Moreover, in order to permit the turning of the flow the upper right-hand eddy now contains another centre about which the flow turns. With further increases in lid speed the upper left-hand eddy is continuously diminished, although even for $v_0 = 0.1$ it is still present. Since the cavity is shallow, as low a lid speed as 0.01 is sufficient to almost completely erase the effects of thermal convection.

4. Conclusion

We have considered in this paper the combined effects of buoyancy and lid motion on the flow field in a viscous fluid completely filling a rectangular container. When the forces generating the fluid motion are not too strong, the slow motion has been shown to be governed by an inhomogeneous biharmonic equation for the stream function. The forcing here is due to the buoyancy and in this approximation the known temperature field drives the fluid motion. It has been shown that the mixed-

https://doi.org/10.1017/S0022112002002069 Published online by Cambridge University Press

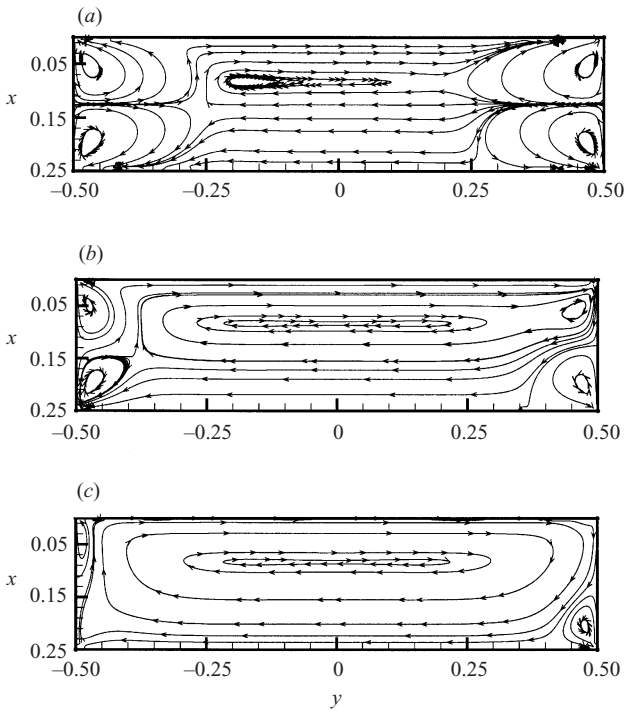


FIGURE 8. Mixed convection in a cavity of depth $D = 0.25$ when the top wall is heated and the bottom wall cooled. (*a*) $v_0 = 0.0001$, (*b*) $v_0 = 0.01$ and (*c*) $v_0 = 0.1$.

convection problem can be conveniently solved by solving a sequence of biharmonic boundary value problems using the natural complex eigenfunctions for this geometry.

Suitable non-dimensionalization shows that the flow field depends on only two parameters: the dimensionless depth and the dimensionless lid speed. In order to illustrate the different phenomena that can occur we have considered four different cases of wall heating and for each case the effects of changing the depth and the lid velocity have been studied. By and large, sidewall heating leads to simple fields whose structures can be inferred from elementary physical reasoning. When the heating or cooling of the top and bottom walls generates the motion, the flow fields are much more complex. Small changes in the wall temperature protocols lead to changes in the eddy topology.

Apart from the interesting and new qualitative features of eddy structure that have been found in this investigation, the detailed results on mixed convection should be useful in examining the possibility of controlling these motion. Specifically, the results presented here suggest the magnitudes of the lid velocities that would be necessary to effect significant changes in the thermally driven circulation. We have not however pursued this idea very far here.

The work reported above was done as a part of the Indo–Ukraine Joint Research Project entitled "Vortex structures and heat transfer in driven cavities". We gratefully acknowledge the support of the Ukrainian and Indian governments. P. N. S. would like to thank Ms D. Shobha for help in the preparation of the manuscript. We would also like to thank an anonymous referee for pointing out that the results for Case D were in error in the first version of this paper.

https://doi.org/10.1017/S0022112002002069 Published online by Cambridge University Press

REFERENCES

Chandrasekhar, S. 1961 *Hydrodynamic and Hydromagnetic Stability*. Oxford University Press.

Jaluria, Y. 2001 Fluid flow phenomena in materials processing – the 2000 Freeman Scholar Lecture. *Trans. ASME* : *J. Fluids Engng* **123**, 173–210.

Joseph, D. D. & Sturges, L. 1975 The free surface on a liquid filling a trench heated from its side. *J. Fluid Mech.* **69**, 565–589.

Liu, C. H. & Joseph, D. D. 1977 Stokes flow in wedge-shaped trenches. *J. Fluid Mech.* **80**, 443–463.

Meleshko, V. V. 1996 Steady Stokes flow in a rectangular cavity. *Proc. R. Soc. Lond.* A **452**, 1999–2022.

Moffatt, H. K. 1964 Viscous and resistive eddies near a sharp corner. *J. Fluid Mech.* **18**, 1–18.

Pan, F. & Acrivos, A. 1967 Steady flows in rectangular cavities. *J. Fluid Mech.* **28**, 643–655.

Pozrikidis, C. 1992 *Boundary Integral and Singularity Methods for Linearized Viscous Flow*. Cambridge University Press.

Shankar, P. N. 1993 The eddy structure in Stokes flow in a cavity. *J. Fluid Mech.* **250**, 371–383.

Shankar, P. N. & Deshpande, M. D. 2000 Fluid mechanics in the driven cavity. *Annu. Rev. Fluid Mech.* **32**, 93–136.

Srinivasan, R. 1995 Accurate solutions for steady plane flow in the driven cavity. *Z. Angew Math. Phys.* **46**, 524–545.

Tuann, S.-Y. & Olson, M. D. 1978 Review of computing methods for recirculating flows. *J. Comput. Phys.* **29**, 1–19.

Yu, K. M. & Nansteel, M. W. 1990 Buoyancy-induced Stokes flow in a wedge-shaped enclosure. *J. Fluid Mech.* **221**, 437–451.

https://doi.org/10.1017/S0022112002002069 Published online by Cambridge University Press